ELSEVIER

Chemical Engineering Journal 89 (2002) 89–99

Chemical Engineering Journal

www.elsevier.com/locate/cej

Rigorous design of extended fully thermally coupled distillation columns

Young Han Kim*

Department of Chemical Engineering, Dong-A University, 840 Hadan-dong, Saha-gu, Pusan 604-714, South Korea

Received 6 August 2001; received in revised form 5 April 2002; accepted 13 May 2002

Abstract

An approximate design procedure of extended fully thermally coupled distillation columns (FTCDCs) is refined for the design of real system having non-ideal equilibrium relation. For high thermodynamic efficiency and reduced computational load, a structural design utilizing the minimum tray structure is implemented, and the design procedure to find operational variables for a given specification of products is explained in detail. The thermodynamic efficiency of several structures of the extended FTCDC is examined from their distillation lines adopted from the residue curve of equilibrium distillation having ideal efficiency. With the structure of the highest efficiency among various ones, the proposed design is applied to three real systems of different chemical groups. The design outcome of the systems shows the effectiveness of the proposed design procedure.

Keywords: Thermally coupled distillation; Extended Petlyuk column; Structural design; Thermodynamic efficiency; Minimum flow computation

1. Introduction

Higher thermodynamic efficiency of a fully thermally coupled distillation column (FTCDC), also known as the Petlyuk column, than the efficiency of a conventional distillation system has widely been recognized ever since it was introduced a half century ago. The high efficiency has been proved in the field applications [1–3] of several chemical companies as well.

Comparing the distribution of liquid composition in the FTCDC with a diagram of residue curves indicates their resemblance [4,5]. One of the residue curves matches the liquid composition profile of a packed distillation column in total reflux operation, where the thermodynamic efficiency of the distillation associated with the curve is ideal. When the liquid profile of a distillation system follows one of the residue curves, the efficiency of the system is predicted to be high. The fact that the profiles of the FTCDC and the extended FTCDC are close to the residue curves gives the answer for the high efficiency of the columns. While the FTCDC consisting of a main column and a pre-fractionator is for the separation of a ternary mixture, the extended FTCDC having a main column and two satellite columns is for a quaternary mixture.

An early study on the structure of the extended FTCDC had been conducted by Sargent and Gaminibandara [6]. Kaibel [7] improved the structure with different arrangement of the sections in the column, and later Agrawal [8] introduced another structure along with the structures for the separation of five and six component mixtures. Christiansen et al. [9], examined the operability of the structures by counting the degrees of freedom, and compared their thermodynamic efficiencies using minimum energy requirement. The study shows that Agrawal's structure is the most efficient.

In addition to the finding of a high efficiency structure, a means of easy operation is proposed by Agrawal [10]. Rearranging the sections of the extended FTCDC for the sequential distribution of column pressure matched with the direction of vapor flow eliminates an external compression of the vapor stream to cope with pressure difference between interlinking trays.

Dünnebier and Pantelides [11], utilized rigorous process models for the optimal design of the original and extended FTCDCs. A rigorous simulation employing non-linear equilibrium is used in the search of the minimum of investment and operational costs. When an optimal structure of the column is not preliminary given in the design procedure, the optimization variables include both structural and operational information to become a time-consuming process. Moreover, some sections of the column are eliminated during the search of the minimum cost, and a discontinuous

* Tel.: +82-51-200-7723; fax: +82-51-200-7728.
E-mail address: yhkim@mail.donga.ac.kr (Y.H. Kim).

1385-8947/02/$ – see front matter
PII: S1385-8947(02)00086-4

Nomenclature

A	coefficient matrix in Eq. (11)
C	coefficient vector in Eq. (11)
F	feed flow rate (mol/h)
F1	feed number 1
H	vapor enthalpy (J/mol)
h	liquid enthalpy (J/mol)
K	equilibrium constant
L	reflux flow rate (mol/h)
NF	feed tray number
NP	side draw tray number
NR	location of upper side stream
NS	location of lower side stream
NT	number of trays
S1	system number 1
T	tray temperature (°C)
V	vapor flow rate (mol/h)
X	liquid composition matrix in Eq. (11)
x	liquid composition (mole fraction)
y	vapor composition (mole fraction)
z	feed composition (mole fraction)

Greek letters

α	relative volatility
β	split ratio of component B to the top of column II
γ	split ratio of a component to the top of column I
φ	solution of Underwood equation

Superscript

M	minimum

Subscripts

A	component A
B	component B
C	component C
D	component D
i	component *i*
n	tray number
s	side stream
1	column I
2	column II
3	column III

relation between tray numbers and operational variables is given to result in a complicated problem to be solved. A tray bypass is implemented to deal with the problem [12]. As different approaches, superstructure design techniques were proposed by Agrawal [8] and Caballero and Grossmann [13], which give an answer for the optimal structure of thermally coupled distillation columns and greatly reduce the computational load in the optimal design of the systems.

Current design procedures of the extended FTCDC require a lot of iterative computations because of many degrees of freedom in the design and operation of the column. A commercial design package, for example, provides the liquid composition profile only for a given structure. Therefore, lots of iterative computations have to be conducted to find the optimal structure. Recently developed optimal design procedures including structural variables in the optimization are also not free from the heavy computational load.

An approximate design procedure giving the optimal structure of an extended FTCDC to reduce the computational burden has been proposed and applied to example systems with ideal equilibrium [14]. In this study, the extension of the procedure for rigorous design is explained and implemented to three example systems for the evaluation of the design performance. From the outcome of the rigorous design, the initial process values for a dynamic simulation of the column can be obtained for the further study of column operation. In order to explain high thermodynamic efficiency of the structure of this study, the efficiency of several known structures is examined comparing their distillation lines with residue curves.

2. Degrees of freedom analysis

The extra degrees of freedom of an extended FTCDC give a variety of operational alternatives in the production of specified products. But the extra degrees incur lots of operational difficulties. Though many manipulated variables are available for preferred controlled variables, product specification in most cases, a distinctive pairing between the manipulated and controlled variables is not simple as shown in the control scheme design of an FTCDC [1]. This indicates that the operation of the extended FTCDC is tough, and one of obstacles for its wide application is from the difficulty.

There are several different arrangements of the extended FTCDCs. One of the arrangements is illustrated in Fig. 1, which has one reboiler and one condenser to separate four components. The arrangement is the same as Agrawal configuration [8] of a main column and two satellite columns, though top and bottom sections of the main column are moved to the satellite columns. A degrees of freedom analysis is conducted by Kim [14], and it is found that there are 18 degrees of freedom. The outcome is utilized in the design of this study. Among them, 10 structural design variables—the numbers of stages of a main column and two satellite columns, feed and two side product locations and four interlinking stages between the main column and satellite column—and six operational variables—reflux flow rate, vapor boil-up rate, two liquid split ratios from the highest column to the top of the next column in two steps and two vapor split ratios from the lowest column to the bottom of the next higher column—are determined from the design of the extended FTCDC after 2 degrees of

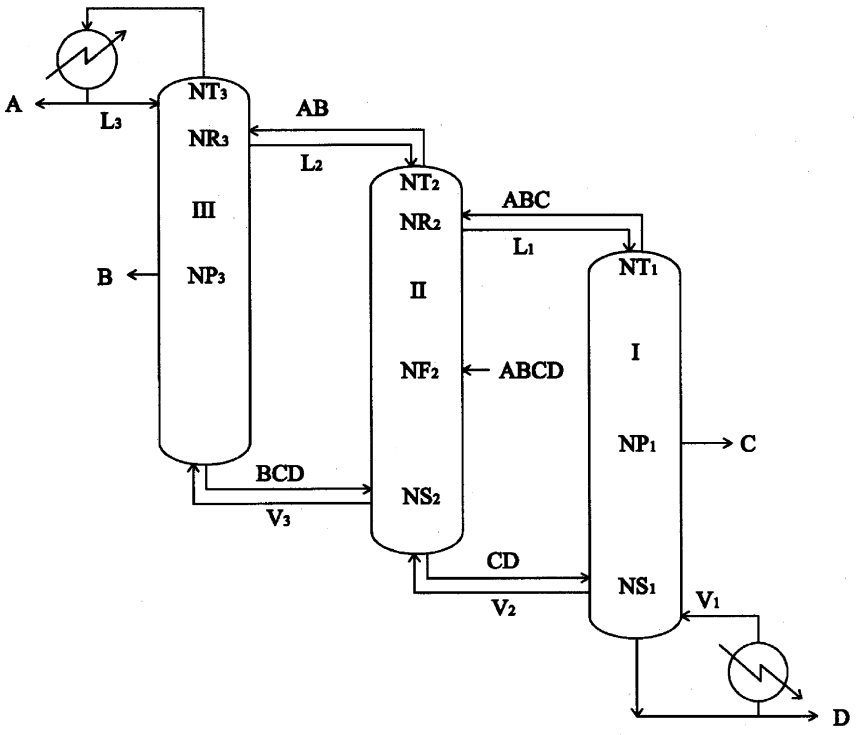

Fig. 1. Schematic diagram of a modified extended FTCDC.

freedom are reduced from the 18 with the assumption of tight inventory control in a reboiler and a reflux drum.

3. Analysis of various structures

A diagram of residue curves for a quaternary system is illustrated in Fig. 2. Owing to the difficulty to illustrate the liquid composition profile for an extended FTCDC with a three-dimensional diagram like Fig. 2, a two-dimensional projection of the profile is employed in the following explanation. Because the figure is drawn in two-dimensional scale, an accurate representation of all the four components for a mixture on the curve is not available. Instead, the closeness to one of corners of the rectangular figure indicates relatively high concentration of the corner component.

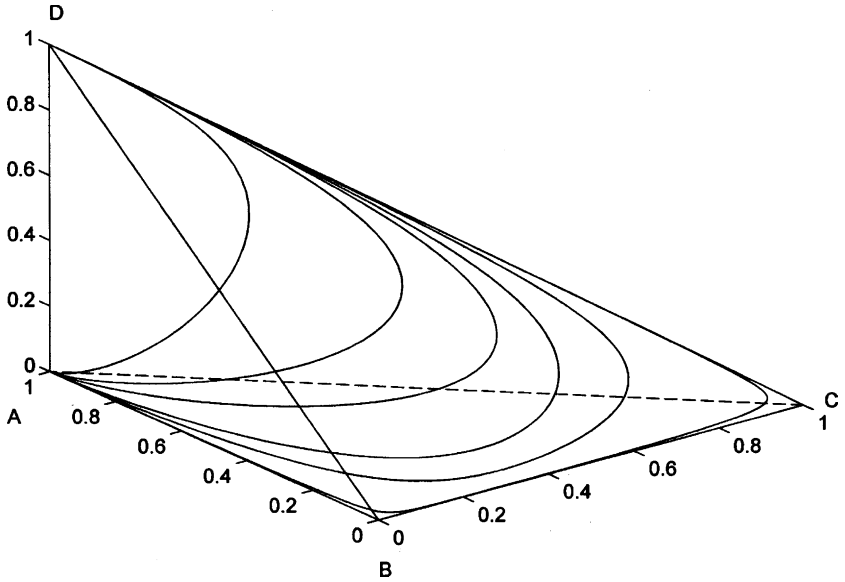

Fig. 2. Residue curves of a quaternary system.

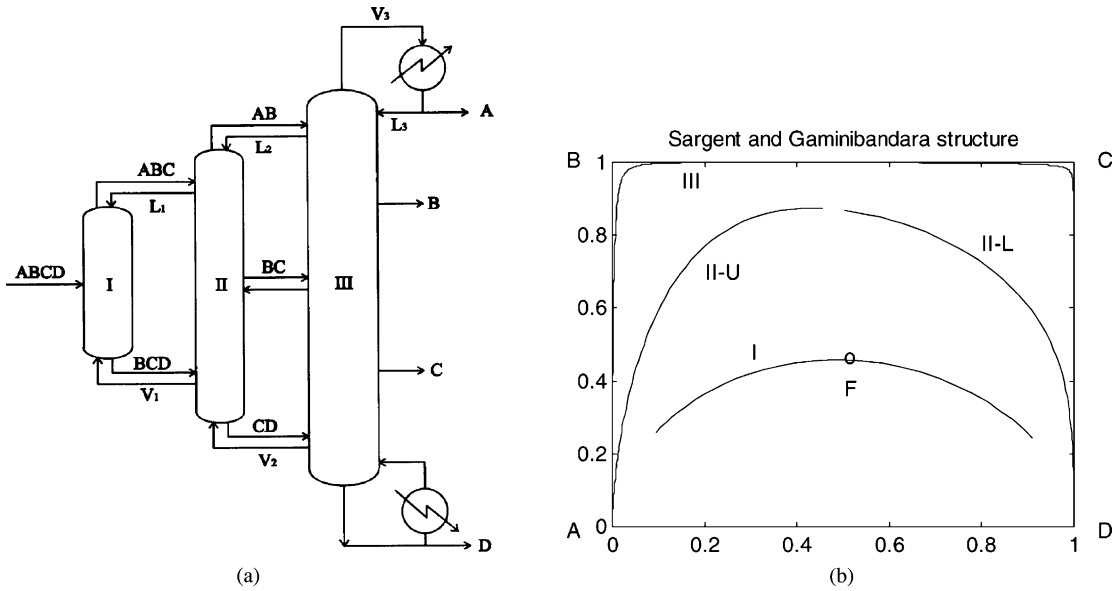

Fig. 3. Schematic of Sargent and Gaminibandara arrangement for quaternary separation and liquid composition profile.

When the profile of liquid composition distribution of an extended FTCDC follows one of the residue curves, the thermodynamic efficiency of the column is ideal. It is because the residue curves denote the composition profile for a packed distillation column in total reflux operation [15]. Though the residue curves represent the liquid composition profile of a packed column, it is generally assumed that they are accurate representations of the profile of a tray column at total reflux [15–17]. Note that the shape of the composition profile of a tray column is similar to the curves. Thus, comparing the composition profile of the extended FTCDC with the residue curves tells how efficient a certain structure of the column is. The liquid composition profile of Sargent and Gaminibandara's column [6] is shown in Fig. 3 along with its structural description. The *F* of column I in Fig. 3(b) denotes feed composition. The curves in the figure are liquid composition profiles adopted from the residue curves. The interlinking of the first and the second columns is made near to the left and right ordinates, respectively, but the locations of the first column are not so close to the ordinates. In other words, some mixing occurs in the interlinking trays. The second and the third columns are interlinked with higher composition of A or D component, and they prevent from close interlinking between columns I and II. In addition, the

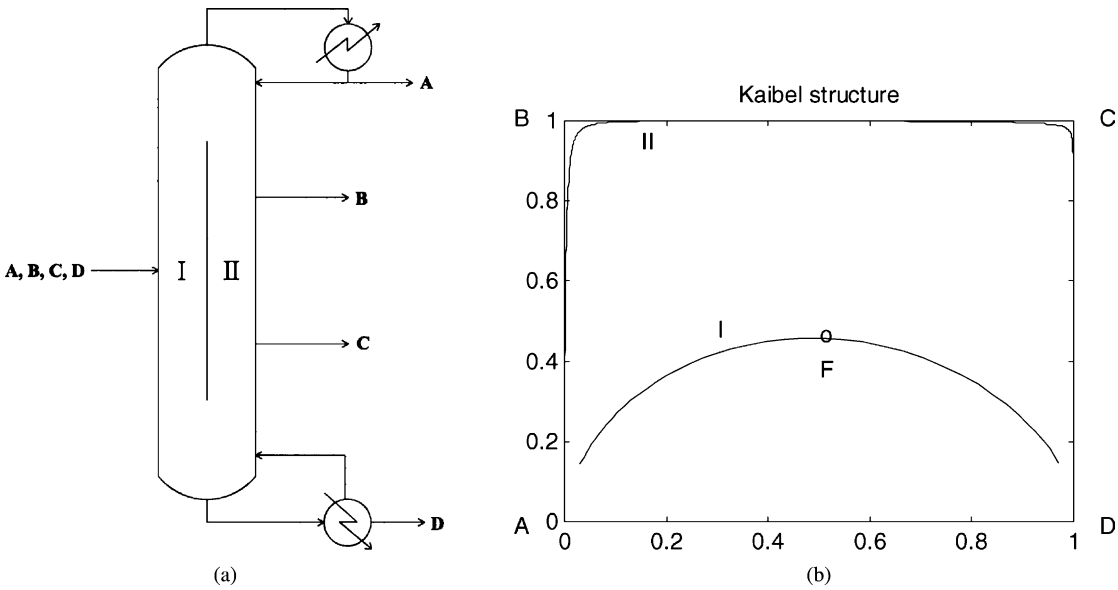

Fig. 4. Schematic of Kaibel arrangement for quaternary separation and liquid composition profile.

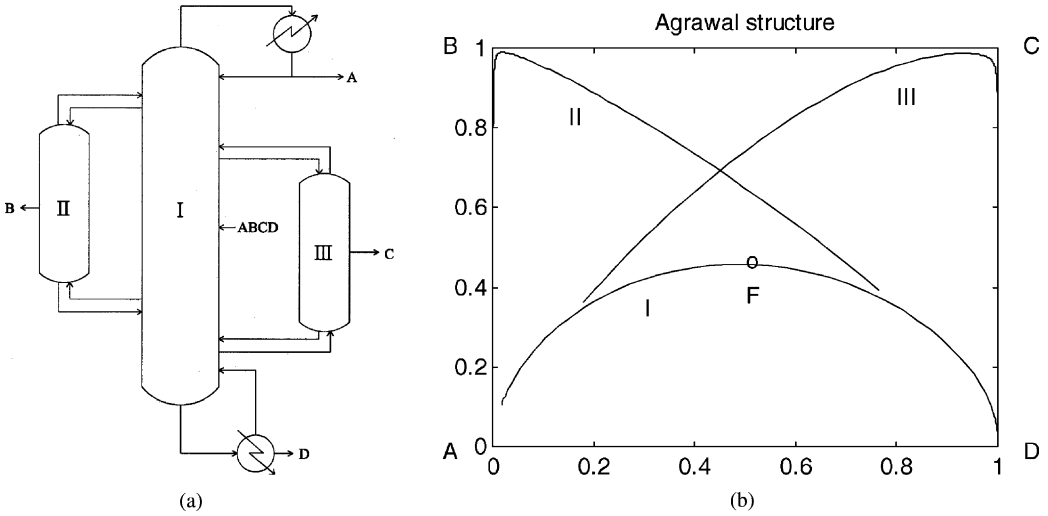

Fig. 5. Schematic of Agrawal arrangement for quaternary separation and liquid composition profile.

middle of the second column is linked to the third column. In this arrangement, there is another composition difference between the interlinking trays to result in mixing. The mixing is an irreversible process and reduces the thermodynamic efficiency of the column. In order to lower the mixing, the upper interlinking between the first and the second columns can be made at the location near to component A, but it is impossible for component B to be transported from column I to II through the interlinking at the location. Therefore, the composition discrepancy at the interlinking trays is inevitable with the structure. In the diagram of Kaibel's column, as shown in Fig. 4, the composition difference in interlinking trays is even greater than that of the Sargent and Gaminibandara's column. Though all the components of A and B have to be transported through the upper interlinking, close connections are only available near to the corner of components A. Because the composition of component B in the interlinking stream is higher than the Sargent and Gaminibandara's column, the connection from the left-hand side of the divided section denoted as I in Fig. 4(b) is far from the right-hand side of the section marked as II and there has to be a large composition difference between the interlinking trays. It means that large irreversible mixing occurs at the interlinking to result in low column efficiency.

Meanwhile, Agrawal's column, as given in Fig. 5, does not produce large composition difference at the interlinking trays. The proper arrangement of distillation column sections leads to close interlinking between the main and two satellite columns as shown in the liquid composition profiles in Fig. 5(b). The profiles are distillation lines drawn from the residue curves. There is little mixing in this arrangement. An efficiency comparison [9] of the three structures in Figs. 3–5 indicates that the Agrawal's column has the highest efficiency, the Sargent and Gaminibandara's column is the next, and the Kaibel's is the lowest. This implies that the structural analysis using the composition profile derived from the residue curves is useful to predict column efficiency and to devise a new column structure.

4. Structural design

Most of design procedures utilizing rigorous process model and commercial design packages for an extended FTCDC do not search the optimal column structure. Instead, they iteratively calculate product compositions until desired products are yielded with given structure of the column. Because there are 10 degrees of freedom concerning the column structure, many different sets of the structure have to be examined to see if one of them gives the optimum cost of column construction and operation. On the other hand, a structural design procedure giving the optimal structure helps to eliminate the iterative searching. Hence, the proposed design procedure of the extended FTCDC follows an approximate design procedure including the structural design [14].

When the composition profile of the extended FTCDC matches one of residue curves, the thermodynamic efficiency of the column is ideal because the curve represents a column of total reflux operation and ideal tray efficiency. The structure of the minimum trays of the extended FTCDC similar to Fig. 5 satisfies the requirement, and a practical column of the same structure is optimal. The minimum tray is for an ideal column operation with infinite reflux ratio.

The minimum number of trays of the extended FTCDC are found from the stage-to-stage computation. Assuming that the feed tray has the same liquid composition as that of a saturated liquid feed and tray efficiency is ideal, one can calculate the liquid composition of the stages above the feed tray from Eq. (1).

$$x_{n+1,i} = \frac{K_{n,i}x_{n,i}}{\sum_j K_{n,j}x_{n,j}} \quad (1)$$

where the subscript n denotes the nth tray counted from bottom and the subscript i denotes the component i. The K is an equilibrium constant, which is computed from a non-ideal equilibrium relation. The UNIQUAC equation is used in this study. The stage-to-stage computation continues past the presumed upper interlinking composition of which the determination is given later.

Similarly, the liquid composition of the stages below the feed tray is found in the stage-to-stage manner using,

$$x_{n-1,i} = \frac{x_{n,i}}{K_{n-1,i}\left[\sum_j (x_{n,j}/K_{n-1,j})\right]} \quad (2)$$

While the computation of Eq. (1) is straight forward, that of Eq. (2) is different because the equilibrium constant has an implicit information. A simple optimization is necessary to find the one stage below composition satisfying Eq. (2).

The stage-to-stage calculation for columns I and III in Fig. 1 is exactly the same as the above except that the compositions of two side products are utilized as the beginning composition instead of the feed composition. The calculation for lower section of the column I continues until the bottom product composition is found. Obviously, the overhead product composition is yielded from the evaluation of the upper section of column III. The specification of key component in overhead and bottom products is 0.975 mole fraction, and that of two side products is 0.95 mole fraction. The stages of feed and two side products are readily determined from the result of tray composition computation.

The locations of interlinking among three columns are decided by matching the compositions between two interlinking trays as shown in Fig. 1. In order explain the selection process of interlinking trays, the computation result of stage-to-stage liquid composition for the example system of S1 with feed F1 is listed in Table 1. From the feed column, column II in Fig. 1, the top tray (NT_2) is set to stage 4, which is interlinked with the tray NR_3 in column III. The next, stage 5, has closer match with the stage 11 in the column III, but the interlinking stage in the column III is too close to the top of the column to handle the component C contained in the stream from the column II. This consideration is also applied to the selection of bottom, stage 3, in the lower section of the column II. In the determination of the interlinking tray NR_2, stages 1 and 3 are not suitable because they are too close to the tray of either feed or column top. When the stage 2, the only choice, is compared with the stages in the upper section of column I for interlinking, the stage 7 of the column I is the best pair. Considering feed and bottom trays in the lower section of the feed tray the interlinking tray NS_2 is set to the middle of stage 1 and 2 because either one of them is too close to the feed tray or bottom. Likewise, the bottom of column III is determined to be in between stages 5 and 6.

As a result, all the 10 structural variables are decided by taking twice the numbers of trays for three columns. For instance, the minimum tray number of the feed column is

Table 1
Result of stage-to-stage composition computation and selection of interlinking stages

	Stage	A	B	C	D	Remarks
Feed column (II)						
Upper	0	0.250	0.250	0.250	0.250	
	1	0.518	0.287	0.137	0.059	
	2	0.716	0.226	0.050	0.009	NR_2
	3	0.826	0.157	0.016	0.001	
	4	0.888	0.107	0.005	0.000	NT_2
	5	0.925	0.073	0.001	0.000	
Lower	0	0.250	0.250	0.250	0.250	NS_2
	1	0.071	0.125	0.251	0.553	
	2	0.014	0.043	0.167	0.777	Bottom
	3	0.002	0.012	0.092	0.893	
	4	0.000	0.003	0.047	0.949	
Light side column (III)						
Upper	0	0.025	0.950	0.024	0.001	
	1	0.047	0.942	0.011	0.000	
	2	0.085	0.910	0.005	0.000	
	3	0.149	0.849	0.002	0.000	
	4	0.247	0.752	0.001	0.000	
	5	0.379	0.621	0.000	0.000	
	6	0.526	0.474	0.000	0.000	
	7	0.661	0.339	0.000	0.000	
	8	0.767	0.233	0.000	0.000	
	9	0.842	0.158	0.000	0.000	
	10	0.893	0.107	0.000	0.000	NR_3
	11	0.927	0.073	0.000	0.000	
	12	0.950	0.050	0.000	0.000	
	13	0.965	0.035	0.000	0.000	
	14	0.976	0.024	0.000	0.000	NT_3
Lower	0	0.025	0.950	0.024	0.001	Bottom
	1	0.013	0.932	0.050	0.005	
	2	0.007	0.873	0.099	0.021	
	3	0.003	0.734	0.176	0.087	
	4	0.001	0.485	0.242	0.271	
	5	0.000	0.224	0.225	0.550	
	6	0.000	0.076	0.150	0.774	
Heavy side column (I)						
Upper	0	0.001	0.024	0.950	0.025	
	1	0.004	0.048	0.937	0.011	
	2	0.012	0.093	0.890	0.005	
	3	0.039	0.170	0.790	0.002	
	4	0.113	0.273	0.614	0.001	
	5	0.265	0.354	0.380	0.000	
	6	0.475	0.349	0.175	0.000	
	7	0.662	0.275	0.063	0.000	NT_1
	8	0.787	0.193	0.020	0.000	
Lower	0	0.001	0.024	0.950	0.025	
	1	0.000	0.012	0.934	0.054	
	2	0.000	0.006	0.884	0.111	
	3	0.000	0.002	0.784	0.213	
	4	0.000	0.001	0.631	0.369	
	5	0.000	0.000	0.446	0.554	
	6	0.000	0.000	0.277	0.723	
	7	0.000	0.000	0.155	0.845	
	8	0.000	0.000	0.081	0.919	NS_1
	9	0.000	0.000	0.041	0.959	
	10	0.000	0.000	0.020	0.980	Bottom

Table 2
Design result of the example systems

System	Feed	NT_1	NT_2	NT_3	NS_1	NP_1	NF_2	NR_2	NS_2	NP_3	NR_3	L_1	L_2	L_3
S1	F1	35	16	41	4	21	10 (7)	11	4	12	37 (32)	172	211	443
S2	F1	46	22	59	4	20	8	14	4	13	43 (41)	192	221	457
S3	F1	49	15	44	4	26	11 (9)	12	5	14	43 (40)	242	286	586
	F2	49	11	44	4	26	9	10	4	14	43 (40)	197	236	523
	F3	49	16	44	5	26	12 (10)	13	4	14	40	194	232	486

taken to be eight from four of upper section, three of the lower section and feed tray itself. Twice of the number, 16, is shown in Table 2 and all others are computed in the same manner. Some of them are adjusted to satisfy the product specification, in which the numbers in parentheses are the original tray numbers computed from the minimum design. Note that the stage numbers in Table 1 is of the minimum structure and those of Table 2 are of the actual columns. From the procedure, the total numbers of trays of the three columns are determined at the same time, and all the 10 structural variables are decided without an optimum searching. The result of the structural design of the minimum tray for the basic example system is demonstrated in Fig. 6.

Notice that the structure from the proposed design leads to high thermodynamic efficiency because the profile of liquid composition of the whole system is based on the minimum trays. In the design of a practical column, proportionally increasing all the numbers makes the structure sustained to keep the high efficiency. Though the tray numbers are increased by the factor of two, the structure remains in the optimum. This practice is implemented in the design of a binary distillation column, such as the McCabe–Thiele design [18]. There is an optimum ratio between the practical and the minimum columns for the lowest cost of investment and operation [19]. In this study, however, a ratio of 2 is adopted from literature [20,21], which is within the range used in industrial practice. The relation between reflux ratio and tray number indicates that while the reflux ratio varies between 1.1 and 1.5 times the minimum, the tray number is between 1.7 and 2.6 times the minimum tray number. For the commonly used reflux ratio of 1.3 times the minimum reflux, the twice the minimum tray is a reasonable design for a usual distillation column [21]. The outcome of the structural design for the example systems of this study is listed in Table 2, symbols of which are given in Fig. 1.

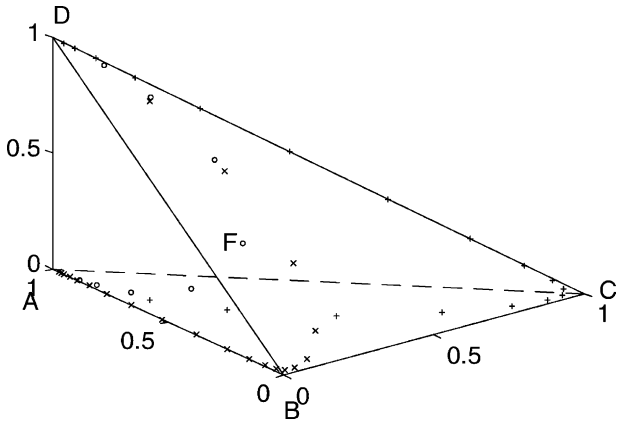

Fig. 6. Liquid composition profile in an extended FTCDC system with a minimum number of trays.

The practical column having finite amount of reflux employs more than the minimum trays. In this situation, the liquid composition of feed tray may not be equal to feed composition and a composition discrepancy occurs. In addition, though the structure of the practical column is same to the minimum tray, the ideal tray liquid composition—equal to the vapor composition of one stage below—is not valid any longer with the finite reflux flow and the feed tray composition does not necessarily match to the feed composition.

5. Operational decisions

From the analysis of degrees of freedom, 18 degrees are found and the structural design gives the answer for the 10 of them. Tight inventory controls at reboiler and reflux drum reduce the degrees by 2. Therefore, six operational variables—reflux flow rate, vapor boil-up rate, two liquid split ratios and two vapor split ratios between a main column and two satellite columns—are to be obtained from the following procedure.

The optimum transfer of components B and C is derived in the calculation of the minimum liquid flow rates for the three columns in Fig. 1. For the simplicity of explanation, Fig. 3(a) is utilized. From column I, components B and C go to column II through either top or bottom of the column. Let the portion of component B from the top of the column be γ_B and component C be γ_C, and their definitions are given by Kim [14].

Similarly, the ratio of component B from the top of column II to III, β, is defined from Fidkowski and Krolikowski [22]. When these optimum transfer ratios for components B and C are utilized, two vapor splits are calculated from material balances and four remaining variables are to be evaluated from steady-state simulation. The initial values of reflux flow rate and liquid split ratios are derived from the minimum liquid flow, but a search for the split ratios has to be conducted because the minimum is too conservative [23]. The sensitivity of vapor and liquid split ratios on the

product composition is not so significant [1,24] that the ratios are not employed as a manipulated variable to control product composition [25–27].

The minimum liquid flow in column I is derived in Fidkowski and Krolikowski [22],

$$L_1^{\mathrm{M}} = \frac{\alpha_{\mathrm{D}} F}{\alpha_{\mathrm{A}} - \alpha_{\mathrm{D}}} \tag{3}$$

From the optimum split ratios, the vapor flow in column I is:

$$V_1^{\mathrm{M}} = L_1^{\mathrm{M}} + Fz_{\mathrm{A}} + Fz_{\mathrm{B}}\gamma_{\mathrm{B}} + Fz_{\mathrm{C}}\gamma_{\mathrm{C}} \tag{4}$$

Using the Underwood equation [28], the minimum vapor flow in column II is found as:

$$V_2^{\mathrm{M}} = \frac{\alpha_{\mathrm{AC}} Fz_{\mathrm{A}}}{\alpha_{\mathrm{AC}} - \varphi} + \frac{\alpha_{\mathrm{C}} Fz_{\mathrm{B}}\beta}{\alpha_{\mathrm{BC}} - \varphi} \tag{5}$$

Then, the minimum liquid flows of columns II and III are given as [14]:

$$L_2^{\mathrm{M}} = V_2^{\mathrm{M}} - Fz_{\mathrm{A}} - Fz_{\mathrm{B}}\gamma_{\mathrm{B}}\beta \tag{6}$$

and

$$L_3^{\mathrm{M}} = \frac{\alpha_{\mathrm{AB}} Fz_{\mathrm{A}}}{\alpha_{\mathrm{AB}} - \varphi} - Fz_{\mathrm{A}} \tag{7}$$

Note that the minimum flow rates are only used in the evaluation of the initial set of operational variables. For a given vapor boil-up rate and liquid flow rates of three columns, a steady-state simulation is conducted to find the product compositions. If the compositions do not satisfy the specification, different liquid flow rate is applied until the specified product is yielded. The increase of reflux flow rate, L_3, raises the composition of the lightest component in overhead product. It also reduces the composition in side draws, which means the elevation of the composition of the major component in the products. Therefore, the selection of new flow rate is determined from consulting the currently calculated composition of overhead product and given specification. The computation path for the design of operating condition in the example case of system S1 with feed F1 is listed in Table 3. The product composition is of key component. The minimum values are calculated first, and the set of operation condition is derived from the minimum values with an initial trial flow rate of L_3. Then, the liquid flow is raised to meet the given product specification. The split of liquid flow is also adjusted by considering the variation of computed product composition. During the determination of the split, the optimum is found from the condition of the highest product composition. The flow of V_1 is set from the amount of bottom product.

Table 3
Computation result in the design of operating condition

Step	L_3	V_1	L_2	L_1	x_{A}	x_{B}	x_{C}	x_{D}
Minimum	60	55	36	13				
1	300	275	182	65	0.884	0.695	0.579	0.900
2	400	351	200	170	0.951	0.877	0.909	0.934
3	450	396	210	170	0.954	0.938	0.955	0.985
4	443	387	211	172	0.977	0.952	0.965	0.975

6. Steady-state simulation

A rigorous process model is employed in steady-state simulation to calculate product composition for the extended FTCDC having the structure found from the structural design. The model is composed of material and energy balances, and equilibrium relation.

A steady-state material balance for component *i* at the *n*th stage of a column is:

$$L_n x_{n,i} + V_n y_{n,i} = L_{n+1} x_{n+1,i} + V_{n-1} y_{n-1,i} + L_{\mathrm{s}} x_{\mathrm{s},i} + V_{\mathrm{s}} y_{\mathrm{s},i} \tag{8}$$

where the subscript s indicates other streams that flow from or to the adjacent trays. Top and bottom trays, feed and side draw trays, and interlinking trays have the streams. The sign of the last two terms may vary according to flow direction. An energy balance is:

$$L_n h_n + V_n H_n = L_{n+1} h_{n+1} + V_{n-1} H_{n-1} + L_{\mathrm{s}} h_{\mathrm{s}} + V_{\mathrm{s}} H_{\mathrm{s}} \tag{9}$$

where the subscript s denotes the same meaning as in the material balance. The UNIQUAC equation is used as the equilibrium relation in this study, and the binary parameters for the equation is obtained from the HYSYS database. In the computation of liquid composition, an iterative procedure utilizing matrix form of the material balances is employed. For the formulation, the vapor composition in the material balance is replaced with a liquid composition and an equilibrium constant. The constant is found from the equilibrium relation and is renewed when new liquid composition is available in the iterative computation.

$$y_{n,i} = K_{n,i} x_{n,i} \tag{10}$$

In a matrix form, the material balance is formulated as

$$\begin{bmatrix} \boldsymbol{A}_{11} & \boldsymbol{A}_{12} & \boldsymbol{A}_{13} \\ \boldsymbol{A}_{21} & \boldsymbol{A}_{22} & \boldsymbol{A}_{23} \\ \boldsymbol{A}_{31} & \boldsymbol{A}_{32} & \boldsymbol{A}_{33} \end{bmatrix} \begin{bmatrix} \boldsymbol{X}_1 \\ \boldsymbol{X}_2 \\ \boldsymbol{X}_3 \end{bmatrix} = \begin{bmatrix} \boldsymbol{C}_1 \\ \boldsymbol{C}_2 \\ \boldsymbol{C}_3 \end{bmatrix} \tag{11}$$

where three groups of liquid composition represent three columns of a main column and two satellite columns. The initial liquid composition is assumed to have linear variation along the trays of which end composition is set to the given product specification. Then, the equilibrium constant in Eq. (10) and tray temperature are found from the UNIQUAC equation and the liquid composition. The vapor flow rate of each tray is evaluated from the energy balance, Eq. (9), and the liquid flow rate is from a total material balance. While an approximate design utilizing ideal equilibrium relation employs material balances only in the computation of tray

liquid composition, the introduction of non-ideal equilibrium requires tray temperature and the inclusion of energy balances to find the liquid composition. In addition, the assumption of equimolal overflow is no longer applicable, and the vapor flow rate is computed from the energy balances. Therefore, the whole procedure of the composition calculation becomes much more complicated compared with the approximate design.

Having two coefficient matrices in Eq. (11) resulted from the equilibrium constant and the liquid and vapor flow rates, a new profile is computed from the equation until the tray temperature is converged. The convergence is determined by checking the sum of tray temperature variation, and the limit is set to 0.002 times the number of trays. For the improvement of the convergence, a relaxation is included in the renewal of liquid composition profile. The detail of whole design procedure for the extended FTCDC is given as follows:

(1) Specify F, z_i, x_D, x_B, x_{S1}, and x_{S3}.
(2) Perform stage-to-stage composition calculation.
(3) Get NT, NT_2, NT_3, NF_2, NP_1, NP_3, NR_2, NR_3, NS_1, and NS_2 in minimum trays.
(4) Take twice the minimum as practical trays.
(5) Calculate split ratios of components B and C.
(6) Find the initial liquid split ratio from the minimum liquid flow.
(7) Compute vapor split using the component split ratio.
(8) Provide L_3 and V_1.
(9) Find L_n and V_n using equimolal overflow assumption.
(10) Assume linear composition profile to calculate initial $x_{n,i}$.
(11) Compute equilibrium constant with the UNIQUAC equation.
(12) Obtain new $x_{n,i}$ using matrix inversion.
(13) Calculate h_n and H_n.
(14) Compute V_n from energy balances.
(15) Obtain L_n from material balances.
(16) If the total $|\Delta T_n|$ is greater than limit, go to step 11.
(17) If product compositions do not meet the specification, adjust L_3 and V_1 and go to step 9.
(18) Check if L_3 is minimum. If not, go to step 7 with new liquid split.
(19) Stop.

7. Example systems

In order to examine the performance of the proposed design here, three example systems with equimolar feed and the third system with three different feed compositions are utilized and the result of the design is summarized in Table 2. The three systems are, an alcohol system of methanol–ethanol–1-propanol–1-butanol (S1), an aliphatic hydrocarbon system of *n*-hexane–cyclo-hexane–*n*-heptane–*n*-octane (S2), and an aromatic hydrocarbon system of chloroform–benzene–toluene–chlorobenzene (S3). They are selected from different groups of organic compounds. Feed compositions of the system S3 are equimolar (F1), 0.7–0.1–0.1–0.1 (F2), and 0.4–0.4–0.1–0.1 (F3). The design specification of products for all systems is set to 0.975 of mole fraction of key component in overhead and bottom products and 0.95 of key component in two side products. Feed rate in all cases is 100 mol/h.

8. Results and discussion

The alcohol system (S1) with the equimolar feed (F1) is used as a base system for the following explanation of the design result. Using the stage-to-stage design equations, Eqs. (1) and (2), liquid composition profiles of main and two satellite columns are evaluated for the minimum trays and the compositions are plotted in Fig. 6. A circle denoted "*F*" is feed composition, and the rest of circles represent the composition profile of a main column (column II in Fig. 1). For column I, the profile is given with plus symbols, and the times signs are for column III. At the end of circles near to component D, a plus symbol and the end circle are close and interlinking trays are found from the two. The other end of plus symbol also meets a circle, which leads to another interlinking. Between cross signs and circles, the interlinking trays are obtained in the same manner. By counting the number of symbols, the minimum tray numbers of three columns are found along with location for feed and two side draws.

Taking twice the minimum numbers gives the structural information for a practical distillation system of the extended FTCDC. The steady-state simulation is conducted to find liquid flow rates for the system producing overhead, bottom, and two side products of the specified composition. The computation results for three example systems and three feeds for the third system are summarized in Table 2. Also, the profile of liquid composition of the first system with equimolar feed is demonstrated in Fig. 7. The symbols are the same as in Fig. 6. Generally, the shapes of the

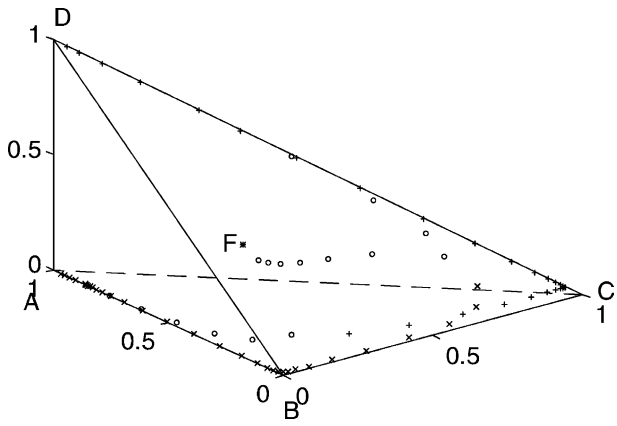

Fig. 7. Liquid composition profile in an extended FTCDC system with a practical number of trays.

composition profile are similar in two figures except that of the main column. There is a mismatch between feed and feed tray compositions. The feed composition is denoted with a star symbol, while the tray composition is the nearest circle. This is common in a practical distillation column, in which more than the minimum number of trays is necessary for the discrepancy. While liquid composition of a tray in the minimum tray of total reflux equals to the vapor composition of the next tray below, the liquid composition in the practical column is different from the vapor. Therefore, the composition of feed tray set to the feed composition in the minimum tray is no longer valid for the practical column. Because of the mismatch, remixing of two middle components is observed in the figure. Unlike Fig. 6, the profile of upper section is curved to component B in Fig. 6. That indicates that the liquid of high composition of component B is remixed to diminish the composition as moving down to feed tray [29]. The same remixing occurs in the lower section of the column.

The table contains tray related numbers from the structural design of practical systems as well. The description of the headings is shown in Fig. 1. The numbers in parentheses are originally calculated numbers from the minimum design, but the specified products are unavailable with the numbers. Mostly the composition of overhead product is too high, and so the upper interlinking location in the column III is moved upward to lower the composition. The composition discrepancy at feed tray also causes some adjustment of feed tray location.

Because the design of this study utilizes the minimum trays of a distillation system, high thermodynamic efficiency is guaranteed. In addition, the computation to find ten variables of structural information required in the design using commercial software is eliminated. The reduction of computational load is significant in the design of the extended FTCDC having many interlinking to result in a lot of design variables.

9. Conclusion

A rigorous design procedure for extended FTCDCs is proposed and implemented to three different real systems. The design is based on the minimum tray structure to give high thermodynamic efficiency by making liquid composition profile similar to the residue curves of equilibrium distillation. Because of the known structure the design becomes simple, while most of field designs utilizing commercial software require a lot of computation to obtain the structure.

The outcome of example system design proves the performance of the proposed design. In addition, the design gives all the process values in the steady-state operation of the designed system, which are utilized as the initial condition of a dynamic simulation of the system for the study of column operation. In the structural analysis, different structures of the extended FTCDC are examine to explain the relation between the distribution of distillation lines and the thermodynamic efficiency of the column.

Acknowledgements

Financial support from the Korea Science and Engineering Foundation through Grant R02-2000-00325 is gratefully acknowledged.

References

[1] E.A. Wolff, S. Skogestad, Operation of integrated three-product (Petlyuk) distillation columns, Ind. Eng. Chem. Res. 34 (1995) 2094–2103.
[2] S. Midori, A. Nakahashi, Industrial application of continuous distillation columns with vertical partition, in: Proceedings of the Fifth International Symposium on Separation Technology between Korea and Japan, Vol. 5, 1999, pp. 221–224.
[3] F. Lestak, D. Egenes, H. Yoda, C. Hamnett, Kellogg divided wall column technology for ternary separation, in: Proceedings of the Fifth International Symposium on Separation Technology between Korea and Japan, Vol. 5, 1999, pp. 233–236.
[4] Y.H. Kim, Rigorous design of full thermally coupled distillation column, J. Chem. Eng. Jpn. 34 (2001) 236–243.
[5] Y.H. Kim, Structural design and operation of a fully thermally coupled distillation column, Chem. Eng. J. 85 (2002) 289–301.
[6] R.W.H. Sargent, K. Gaminibandara, Optimum design of plate distillation columns, in: L.W.C. Dixon (Ed.), Optimization in Action, Academic Press, London, 1976, pp. 267–314.
[7] G. Kaibel, Distillation columns with vertical partitions, Chem. Eng. Technol. 10 (1987) 92–98.
[8] R. Agrawal, Synthesis of distillation column configurations for a multi-component separation, Ind. Eng. Chem. Res. 35 (1996) 1059–1071.
[9] A.C. Christiansen, S. Skogestad, K. Lien, Complex distillation arrangements: extending the Petlyuk ideas, Comput. Chem. Eng. 21 (1997) S237–S242.
[10] R. Agrawal, More operable fully thermally coupled distillation column configurations for multi-component distillation, Trans. IChemE 77 (Part A) (1999) 543–553.
[11] G. Dünnebier, C.C. Pantelides, Optimal design of thermally coupled distillation columns, Ind. Eng. Chem. Res. 38 (1999) 162–176.
[12] H. Yeomans, I.E. Grossmann, Optimal design of complex distillation columns using rigorous tray-by-tray disjunctive programming models, Ind. Eng. Chem. Res. 39 (2000) 4326–4335.
[13] J.A. Caballero, I.E. Grossmann, Generalized disjunctive programming model for the optimal synthesis of thermally linked distillation columns, Ind. Eng. Chem. Res. 40 (2001) 2260–2274.
[14] Y.H. Kim, Structural design of extended fully thermally coupled distillation columns, Ind. Eng. Chem. Res. 40 (2001) 2460–2466.
[15] S. Widagdo, W.D. Seider, Azeotropic distillation, AIChE J. 42 (1996) 96–130.
[16] D.B. Van Dongen, M.F. Doherty, Design and synthesis of homogeneous azeotropic distillations. 1. Problem formulation for a single column, Ind. Eng. Chem. Fundam. 24 (1985) 454–463.
[17] N. Bekiaris, G.A. Meski, C.M. Radu, M. Morari, Multiple steady states in homogeneous azeotropic distillation, Ind. Eng. Chem. Res. 32 (1993) 2023–2038.
[18] W.L. McCabe, J.C. Smith, Unit Operations of Chemical Engineering, 3rd Edition, McGraw-Hill, New York, 1976, p. 548.
[19] M. Van Winkle, Distillation, McGraw-Hill, New York, 1967, p. 242.
[20] K.N. Glinos, M.F. Malone, Design of side stream distillation columns, Ind. Eng. Chem. Process Des. Dev. 24 (1985) 822–828.

[21] J.D. Seader, E.J. Henley, Separation Process Principles, Wiley, New York, 1998, p. 509.
[22] Z. Fidkowski, L. Krolikowski, Thermally coupled system of distillation columns: optimization procedure, AIChE J. 32 (1986) 537–546.
[23] C.J. King, Separation Processes, 2nd Edition, McGraw-Hill, New York, 1980, p. 421.
[24] Y.H. Kim, Design of a fully thermally coupled distillation column based on dynamic simulations, Kor. J. Chem. Eng. 17 (2000) 570–573.
[25] M.I. Abdul Mutalib, R. Smith, Operation and control of dividing wall distillation columns. Part 1. degrees of freedom and dynamic simulation, Trans. IChemE 76 (Part A) (1998) 308–318.
[26] P. Mizsey, N.T. Hau, N. Benko, I. Kalmar, Z. Fonyo, Process control for energy integrated distillation schemes, Comput. Chem. Eng. 22 (1998) S427–S434.
[27] S. Hernandez, A. Jimenez, Controllability analysis of thermally coupled distillation systems, Ind. Eng. Chem. Res. 38 (1999) 3957–3963.
[28] A.J.V. Underwood, Fractional distillation of multi-component mixtures, Chem. Eng. Prog. 44 (1948) 603–614.
[29] C. Triantafyllou, R. Smith, The design and optimization of fully thermally coupled distillation columns, Trans. IChemE 70 (1992) (Part A) 118–132.